THE TRANSLATION OF TURBULENT WIND ENERGY TO INDIVIDUAL CORN PLANT MOTION DURING SENESCENSE*

T. K. FLESCH and R. H. GRANT

Agronomy Department, Purdue University, West Lafayette, IN 47907, U.S.A.

(Received in final form 28 November, 1990)

Abstract. Wind flow within inflexible plant canopies is turbulent and leads to an oscillatory motion of individual plants. A study was conducted to describe the motion of corn (*Zea mays* L.) stalks in the wind using a transfer function in the frequency domain to gain insight into the transfer of energy between the turbulent wind and the corn plant. Plant motion was measured and the wind moment was estimated on 23 plants during six windy days in October 1988, at West Lafayette, IN. Plant motion was theoretically described by a rigid rod. The results showed that lower stalk motion was generally well described by a second-order response model defined by a damping coefficient, natural frequency, and rotary stiffness.

1. Introduction

Wind flow within plant canopies is turbulent and results in plant motion (Inoue, 1955; Maitani, 1979; Holbo *et al.*, 1980). This motion results in a deformation of the plant stem or root system. In some cases, the deformation may exceed the failure limit of the plant and result in stem breakage or uprooting (lodging). A knowledge of the relationship between the turbulent wind energy acting on the plant and plant motion is important in understanding wind-induced lodging, a problem in corn grain production.

Plant motion in the wind is determined by both wind and plant characteristics. Finnigan and Mulhearn (1978) treated wheat (*Triticum aestivum* L.) as a cantilever beam and showed that plant motion was enhanced with increased wind speed, plant density, and plant drag coefficient. The motion was primarily associated with resonant oscillation near the natural frequency (ω_n) of the plant. Maitani (1979; 1981) found that wheat and rice (*Oryza sativa* L.) motion was also characterized by resonant waving.

Holbo *et al.* (1980) studied Douglas-fir (*Pseudotsuga menziesii*) motion in the wind and related it to wind characteristics by a "compliance transfer relation" or "transfer function". Both tree displacement and wind force on the tree were transformed into power spectra ($S_P(f)$ and $S_M(f)$, respectively), and the transfer function $|G(f)|$ calculated as:

$$|G(f)| = [S_P(f)/S_M(f)]^{1/2} .$$

* Published as Paper Number 12,541 of the Purdue University Agricultural Experiment Station.

Boundary-Layer Meteorology **55**: 161–176, 1991.

If a tree was described by a unique $|G(f)|$, its response in the frequency domain could be predicted given the wind characteristics. Holbo *et al.* (1980) suggest that $|G(f)|$ could be a useful tool in reducing windthrow if it was related to plant characteristics and management practices, and used to predict and avoid conditions which are most likely to lead to large strains on a tree.

The objective of this study was to use transfer functions to describe the relationship between the wind energy and wind-induced motion of corn stalks during senescence.

2. Materials and Methods

Wind speed and plant motion measurements were taken within a 0.56 ha corn field at the Purdue University Agronomy Farm, West Lafayette, IN, on 4, 10, 11, 19, 25, and 27 October 1988. Measurement days had wind speeds at 10 m of at least 3 m s^{-1}. Four plants were selected for measurement on each day – two plants within each of two adjacent rows. The four measured plants were contained within an area of approximately 1 m^2 and located at least 45 m from the upwind edge of the field. In total, 23 plants were measured. Measurements were made each day during four 17-min periods.

For analysis, the plants were grouped by ear position (upright or down) and inter-row contact (yes or no). Typically plants have upright ears firmly attached to the stalk before senescence. During senescence, it is common for the ear to fall from the upright position to a "down" position, where the ear is held hanging by the shank. Individual plants were manipulated by taping up or pulling down the ear. Inter-row contact was eliminated by pulling back and securing surrounding plants with elastic cords.

2.1. Plant measurements

Stalk position was measured with a potentiometer-type modified computer joystick (Tandy Corp., Fort Worth, TX, Color Computer Deluxe Joystick Model) attached to the stalk at a height of about 0.6 m (Figure 1). The joystick signals were the active arms of two Wheatstone bridges. The bridge outputs were low-pass filtered at 5 Hz and sampled at 10 Hz by a micrologger data acquisition system (Campbell Scientific Co., Logan, UT, Model CR-21X). The joystick angle in the along-row and the across-row direction was converted to the stalk angle with the vertical. The resolution of the stalk angle was 0.05 to 0.22 deg depending on the geometry of plant attachment. It was assumed that there was no significant rotation of the stalk from either a horizontal torque exerted by the wind or from stalk bending.

One-sided leaf areas, stalk diameters, and plant height were measured on each plant. Stalk diameters at 0.15 m height intervals were calculated by linear interpolation from measurements at 0.08 m, 1.0 m, 1.5 m (2.0 m if the plant height was much greater than 2.0 m), and at the top of the tassel.

The one-sided leaf area distribution with height (LAD) was calculated by parti-

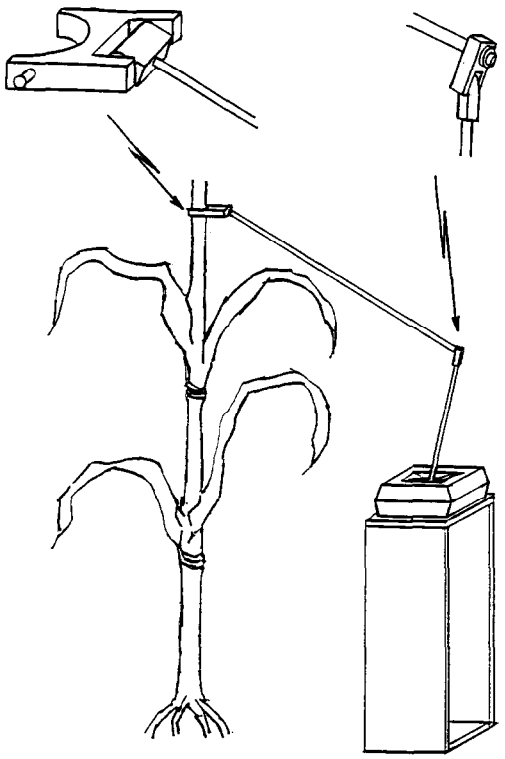

Fig. 1. Illustration of the joystick assembly for measuring the stalk position.

tioning the plant height into 0.15 m increments. The area of each leaf was calculated by multiplying the leaf length by its maximum width and multiplying by 0.75 if the leaf was tapered. The individual leaf area was distributed into three equal lengthwise sections. The area of each third was estimated from the total area of the leaf and the predetermined average proportion of each third to the total area of the leaf. The height of the midpoint of each third was measured and its area added to the total leaf area of the appropriate layer.

2.2. Wind measurements

Within-canopy horizontal wind speed was measured at two heights with constant temperature hot-film anemometers (Thermo Systems Inc., St. Paul, MN, 1050 series). At each height, two hot-film probes (Thermo Systems Inc., St. Paul, Mn, model 1210-20) were arranged in an "X" configuration in a plane parallel to the ground surface. Calculations showed a wind vector oriented 0, 10, 20, and 30 deg from the horizontal would lead to 0, 3, 10, and 23% overestimations of the horizontal speed, respectively.

The hot-film anemometers were placed between the four plants whose position was being measured. The sensors were protected from fluttering leaves by a cylindrical screen cage approximately 0.12 m in diameter and 0.15 m long. The

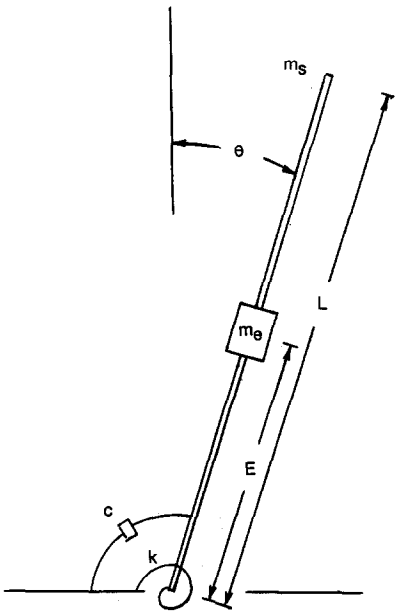

Fig. 2. Rigid rod model of a corn plant illustrating the model parameters.

screen elements were 0.001 m in diameter arranged in a grid spacing of 0.015 m long. The hot-film signals were low-pass filtered with a cutoff frequency of 5 Hz and sampled at 10 Hz by the micrologger system. The hot-film data were corrected for field temperature (Bearman, 1971) and converted to wind speed according to Jorgensen (1971). The horizontal wind speed profile with height was estimated by assuming a linear profile that was: (a) interpolated between the ground (zero speed) and the lowest anemometer height; (b) interpolated between the two anemometer heights; and (c) extrapolated to the plant top. A negative speed could be extrapolated at the plant top. In these cases the speed was set to zero.

2.3. Plant model

The corn plant was considered a rigid rod (stalk) with a concentrated mass (ear) midway up the rod. Conceptually the stalk is attached to the soil by a rotary spring and dashpot (viscous damper) as shown in Figure 2. Forces act on the plant as a moment (or torque). The motion of this system is described by:

$$\underset{\text{A}}{(m_e E^2 + m_s L^2/3)\ddot{\theta}} + \underset{\text{B}}{c\dot{\theta}} + \underset{\text{C}}{k\theta} - \underset{\text{D}}{(m_e g E + m_s g L/2)\sin\theta} = M\,,$$

where m_e is the ear mass (kg), m_s is the stalk mass (kg), E is the ear height (m), L is the stalk height (m), g is the gravitational acceleration ($\mathrm{m\,s^{-2}}$), c is the dashpot coefficient ($\mathrm{n\,m\,s\,rad^{-1}}$), k is the spring constant ($\mathrm{N\,m\,rad^{-1}}$), θ is the angle the stalk makes with zenith (rad), $\dot{\theta}$ is the angular velocity of the stalk (rad

s^{-1}), $\ddot{\theta}$ is the angular acceleration of the stalk (rad s^{-2}), M is the applied moment on the stalk (N m).

The term represented by A is the moment due to the angular acceleration of the plant. The B term is the viscous resistance to motion and C is the restoration moment of the plant. The term D is the moment due to gravity when the stalk is displaced from a vertical position. Assuming small displacement about the equilibrium (so that $\sin\theta \simeq \theta$) gives a linearized equation of motion:

$$(m_e E^2 + m_s L^2/3)\ddot{\theta} + c\dot{\theta} + (k - m_e gE - m_s gL/2)\theta = M .$$

If an equivalent plant mass m_p', and plant spring constant K are defined as:

$$m_p' = m_e E^2 + m_s L^2/3 , \tag{1}$$

$$K = k - m_e gE - m_s gL/2 , \tag{2}$$

the equation of plant motion becomes,

$$m_p'\ddot{\theta} + c\dot{\theta} + K\theta = M . \tag{3}$$

This described a linear, single degree-of-freedom (1-DOF), second-order system.

A simple "rigid rod" model was used to describe plant motion rather than a "flexible beam" model because plant displacement was measured at only one point on the stalk. The description of the displacement of a point on a rigid rod is the same as that of a point on a flexible beam oscillating in only the fundamental mode. It seems unlikely that the stalk has significant displacements associated with higher modes.

The wind moment M (height × force) on the plant was calculated for incremental 0.15 m layers and summed as:

$$M = C_{DS}(\rho/2) \sum_{i=1}^{TOP} [h_i |U_i - \dot{\theta}h_i| (U_i - \dot{\theta}h_i) 0.15\, SD_i] + \\ + C_{DL}(\rho/2) \sum_{i=1}^{TOP} [h_i |U_i - \dot{\theta}h_i| (U_i - \dot{\theta}h_i) AL_i] \tag{4}$$

where C_{DS} is the drag coefficient for the stalk, C_{DL} is the drag coefficient for the leaves, ρ is the air density (kg m^{-3}), i is the index identifying 0.15 m layers above the ground, TOP is the index of the top 0.15 m layer, h_i is center height of layer i above the ground (m), U_i is the wind speed at height h_i (m s^{-1}), SD_i is the stalk diameter (m) at the center of section i (the 0.15 represents the length of the stalk section), AL_i is the one sided leaf area within layer i (m^2).

The right-hand side of Equation (4) represents the moment due to the leaf and the stalk area. The M_w was calculated for each set of wind speed measurements (at 10 Hz). The M_w contributed by the area of the ear and tassel was neglected since preliminary calculations showed a maximum ear area contribution less than

8% of the total and the tassel area was negligable. It was assumed that the direction of M_w was constant over time and height in the canopy.

The $(U_i - \dot{\theta}h_i)$ term is the effective wind speed at the plant surface (wind plus the stalk velocity). This assumes that stalk motion is in the same plane as the wind vector, and that stalk displacement is small enough so that the radial velocity multiplied by the height closely approximates the horizontal stalk velocity. Since the wind speed was, in all but one instance, greater than the stalk velocity (typical $\dot{\theta}h_i/U_i$ for peak winds 0.5 to 0.6 and for mean winds 0.01–0.02), we consider only the case where the magnitude of U_i is greater than $\dot{\theta}h_i$. Regrouping Equation (4) and denoting

$$C_D A_i = C_{DL} A L_i + 0.15 C_{DS} S D_i$$

gives

$$M = \rho/2 \sum_{i=1}^{TOP} U_i^2 C_D A_i h_i - \dot{\theta}\rho/2 \sum_{i=1}^{TOP} (2U_i h_i - \dot{\theta}h_i^3) C_D A_i \,. \tag{5}$$

Combining Equation (5) and (3), and denotings M_w as

$$M_w = \rho/2 \sum_{i=1}^{TOP} U_i^2 C_D A_i h_i \,, \tag{6}$$

and regrouping, gives

$$m_p' + \left[c + (\rho/2) \sum_{i=1}^{TOP} (2U_i h_i - \dot{\theta}h_i^3) C_D A_i \right] \dot{\theta} + K\theta = M_w \,. \tag{7}$$

The natural frequency (ω_n) and viscous structural damping coefficient (ζ_s) of a second-order system are:

$$\omega_n^2 = K/m_p' \,, \tag{8}$$

$$\zeta_s = c/(2\omega_n m_p') \,. \tag{9}$$

In the discussion of results, ω (subscripted n or fv) is converted to f by dividing the ω by 2π.

The aerodynamic damping (ζ_a) was described by

$$\zeta_a = \rho/2m_p' \sum_{i=1}^{TOP} (2U_i h_i - \dot{\theta}h_i^3) C_D A_i \,, \tag{10}$$

which represents the energy added/lost from the drag created solely by the stalk velocity. Dividing Equation (7) by m_p', and inserting Equations (8), (9) and (10) gives,

$$\ddot{\theta} + 2\omega_n[\zeta_s + \zeta_a]\dot{\theta} + \omega_n^2\theta = \omega_n^2 M_w/K \,. \tag{11}$$

The major assumptions in using Equation (11) include: (1) the damping (c) and spring coefficients (K) are constant with stalk velocity and displacement, respec-

tively; (2) plant height and plant area distribution with height remain constant as wind speed changes; (3) there is no significant torsion of the stalk; (4) the wind speed at a given height is greater than the stalk velocity; and (5) the wind direction and the plant motion are in the same vertical plane. Given the complex directional characteristics of within-canopy flows and the complex translation of flow direction into M_w direction and plant motion direction, the last assumption is probably the most frequently violated.

The damping coefficient and natural frequency of each plant were calculated from a free vibration test. The free vibration test consisted of displacing the stalk by hand, releasing it, and recording the motion. The test was made during calm periods with displacement recorded at 20 Hz. The ratio of successive peaks in the angular displacement after release (ϕ_1 and ϕ_2) are (see Meirovitch, 1986)

$$\phi_1/\phi_2 = \exp[2\pi\zeta(1-\zeta^2)^{-1/2}]\,. \tag{12}$$

Solving for ζ gives the value for ζ_{fv} (all damping and free vibration values resulting from these measurements are subscripted '*fv*' in this paper). The ζ_{fv} is actually the sum of the structural damping (ζ_s) and the aerodynamic damping (ζ_a) defined as

$$\zeta_a = \rho/(2m_p') \sum_{i=1}^{TOP} \theta h_i^3 C_D A_i\,. \tag{13}$$

The ζ_a defined in Equation (13) differs from that of Equation (10) in that during the free vibration test, $U_i = 0$. It is not possible to separate the aerodynamic damping of Equation (13) from the structural damping in the free vibration tests. If the corresponding time of peaks ϕ_1 and ϕ_2 are t_1 and t_2, the ω_{fv} (in rad s^{-1}) of the system is

$$\omega_{fv} = [2\pi/(t_1 - t_2)][1-\zeta_{fv}^2]^{-1/2}\,, \tag{14}$$

using ζ_{fv} as calculated from Equation (12).

The rotary stiffiness of each plant in the along-row (K_Y) and across-row (K_X) directions was calculated by applying known moments perpendicular to the stalk via a pulley system. A series of masses were applied to the stalk at ear height (common structural reference point), multiplied by the ear height and the gravitational constant, then divided by the angular displacements of the stalk and averaged to give K_Y and K_X.

The C_{DL} was assumed to be 0.2 (den Hartog, 1973; Uchijima and Wright, 1964; Wilson *et al.*, 1982; Wilson and Shaw, 1977). The C_{DS} was assumed to equal 1.0: the approximate value for a cylinder with the major axis perpendicular to the wind flow at Reynold's numbers above 100 (Daily and Harleman, 1966). For a stalk diameter of 0.006 m (typical at the top of the stalk), this corresponds to wind speeds greater than 0.2 m s^{-1}. Air density was calculated from pressure and temperature measurements.

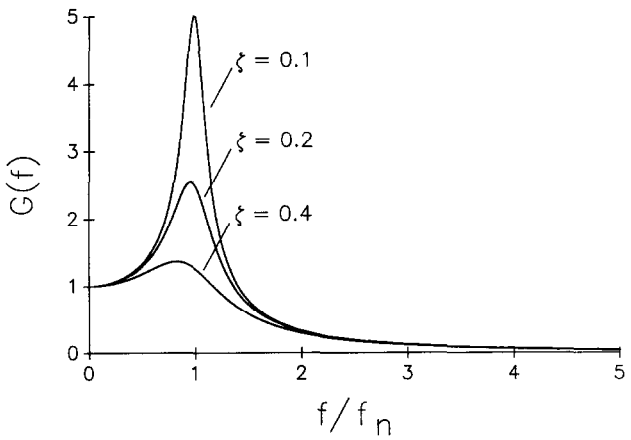

Fig. 3. Theoretical transfer function ($G(f)$) of a second-order system with the ratio of frequency to natural frequency (f/f_n) at three damping coefficients (ζ).

2.4. Time series analysis

Power spectra were calculated for $M_w(S_M(f))$ and the across-row and along-row stalk displacements ($S_X(f)$ and $S_Y(f)$) using a Fast Fourier Transform (FFT) routine (ASYST data analysis package, version 2.01, Macmillan Software Co., New York, NY). Each 17-min measurement period was analyzed in five 2048 point segments. Data in each segment were tapered with a 10% cosine bell function (Bloomfield, 1976), then transformed and emsemble averaged. Numerical integration of the power spectra functions was done using Simpson's 1/3-rule with an interval of 0.0049 Hz.

At any frequency f (Hz), a transfer function gives the ratio of the energy in motion to the excitation energy. The transfer function of a theoretical 1-DOF second-order system, such as the linearized "rigid rod" model is (Meirovitch, 1986)

$$|G(f)| = \{[1 - (f/f_n)^2]^2 + [2\zeta(f/f_n)]^2\}^{-1/2} . \tag{15}$$

This function is illustrated in Figure 3 for various ζ values.

A wind moment-plant motion transfer function $|G_{MP}(f)|$ was calculated from field measurements as

$$|G_{MP}(f)| = K_G[S_P(f)/S_M(f)]^{1/2} ,$$

where

$$S_P(f) = S_X(f) + S_Y(f) .$$

Since a transfer function is generally defined as a non-dimensional ratio of the motion energy to the input energy, and $S_P(f)$ is in units of (deg^2), it was necessary that the ratio of $S_P(f)$ to $S_M(f)$ be multiplied by a stiffness (K_G). The K_G was

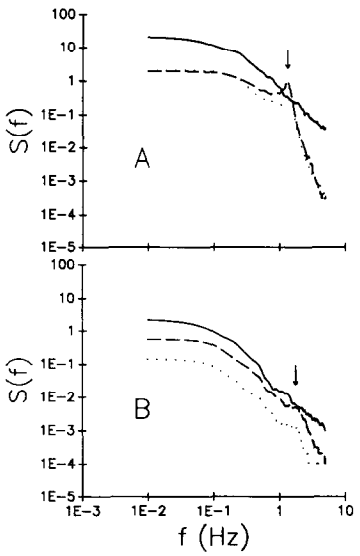

Fig. 4. The power spectra ($S(f)$) of the wind moment (———), and the across-row (-----) and along-row (.....) displacement with frequency (f) for two plants. The measured natural frequency (f_{fv}) is indicated by the arrow (↓).

calculated from the theoretical characteristics of $|G(f)|$. The K_G was selected so that on average the first 20 values of $|G_{MP}(f)|$ (0.0031 to 0.0616 Hz) equaled the values of $|G(f)|$ (Equation (15)).

3. Results and Discussion

3.1. Plant motion and M_w power spectra

Power spectra of $M_w(S_M(f))$, and plant displacement in the cross-row($S_X(f)$) and along-row ($S_Y(f)$) directions followed a similar pattern among the sampled plants (Figure 4). The magnitude of $S_M(f)$ was greatest at the lowest frequencies and decreased continuously as frequency increased. The $S_X(f)$ and $S_Y(f)$ were also greatest at the lowest frequencies. As frequency increased, $S_X(f)$ and $S_Y(f)$ initially declined proportionally with $S_M(f)$, then increased (or the decline slowed) until a frequency near the measured f_n of the plant. This shift in $S_X(f)$ or $S_Y(f)$ near f_n appeared as a sharp peak in some plants (Figure 4A) and as a gentle bulge in others (Figure 4B). The peak in $S_X(f)$ and $S_Y(f)$ near f_n was the result of resonant motion. This was similar to the motion of wheat found by Finnigan (1979) and Maitani (1979), and rice found by Maitani (1981). This indicates that the "Honami waving" of small grains is also present in corn fields.

TABLE I

Statistics for plant damping coefficient (ζ_{fv}), natural frequency (f_{fv}), and plant stiffness (K)

	ζ_{fv}	f_{fv} (Hz)	K (N m deg^{-1})
Mean	0.11	1.54	2.44
Standard deviation	0.03	0.14	1.11
Maximum	0.19	1.80	5.90
Minimum	0.07	1.29	0.64

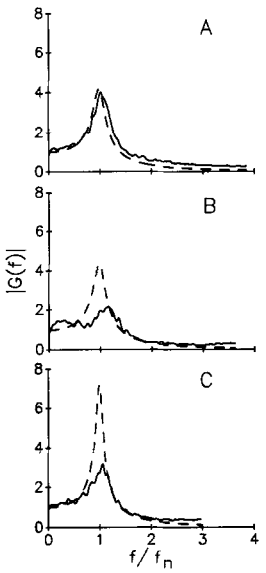

Fig. 5. The measured (——) and theoretical (-----) transfer function ($|G(f)|$) with the ratio of frequency to measured natural frequency (f/f_n) for three plants.

3.2. ζ, f_n, AND K VALUES

The mean, standard deviation, and maximum and minimum values of ζ and f_n determined from free vibration tests (ζ_{fv} and f_{fv}) are shown in Table I. These values were measured on plants where the ear was upright. They represent an average of across-row and along-row direction values. The f_{fv} was relatively constant among the plants measured, with a coefficient of variation (CV) of 8.8%. The f_{fv} had greater variability, with a CV of 26.7%. The mean, standard deviation, and maximum and minimum values of K are also shown in Table I. The K show a larger range of values than either ζ_{fv} or f_{fv}, with a CV of 46%.

3.3. PLANT TRANSFER FUNCTIONS

In general, an isolated plant with an upright ear behaved as a linear, single degree-of-freedom (1-DOF), second-order system. Figure 5 shows comparisons

of the theoretical $|G(f)|$ calculated from ζ_{fv} and f_{fv}, and $|G_{MP}(f)|$ determined from $S_X(f)$ and $S_Y(f)$. Some plants had a $|G_{MP}(f)|$ very close to the theoretical (Figure 5A), while even in the poorest fits (Figure 5B) the general shape of $|G_{MP}(f)|$ matched $|G(f)|$. The maximum values of $|G_{MP}(f)|$ generally did not match the maximum of $|G(f)|$ (Figure 5C). Since the maximum value of $|G(f)|$ depends only on ζ, differences in the maximum of $|G_{MP}(f)|$ and $|G(f)|$ were likely due to differences in the measured ζ_{fv} and the effective ζ.

Equation (15) was fit to the maximum values of $|G_{MP}(f)|$ to give an effective ζ and f_n (ζ_G and f_G). The ζ_G averaged 50% higher than the ζ_{fv}. Some differences in ζ_G and ζ_{fv} was expected due to the nature of aerodynamic damping. During the measurement periods, the wind speed was greater than the stalk velocity at almost all times, and aerodynamic damping is as in Equation (10). During the free vibration test where ζ_{fv} is determined, the stalk velocity is greater than the wind speed, and aerodynamic damping is described by Equation (13). Values of the $2Uh_i$ and $\dot{\theta}h_i^3$ components of aerodynamic damping were estimated for each plant so that the difference in Equations (10) and (13) could be evaluated. For all plants, the contribution of the $\dot{\theta}h_i^3$ term averaged less than 0.1% of ζ_s, while the $2Uh_i$ term averaged 22%. Therefore, the effective damping during windy conditions should be approximately 22%. Therefore, the effective damping during windy conditions should be approximately 22% larger than that found by a free vibration test. The period mean $2Uh_i$ component of damping ranged from 5 to 42% of ζ_s, with instantaneous values as high as 126%.

Since ζ_G averaged 50% greater than ζ_{fv} and the estimated increase in ζ_{fv} due to aerodynamic damping averaged only 22%, it would seem that aerodynamic damping does not explain all of the difference in ζ_{fv} and ζ_G. There are two possible explanations for this. As stalk displacement and stalk velocity were functions of f, it is likely that aerodynamic damping was also a function of f. High stalk velocities associated with plant motion at ω_n would increase aerodynamic damping and result in unexpected decreases in $|G_{MP}(f)|$ at f_n. The difference in ζ_G and ζ_{fv} may also indicate that C_{DL} was higher than the 0.2 used. An increase in C_{DL} would increase aerodynamic damping and reduce the difference in ζ_{fv} and ζ_G. As will be discussed later, there is other evidence that C_{DL} is greater than 0.2.

3.4. Effect of row contact and ear position

There was little difference in $|G_{MP}(f)|$ for plants with inter-row contact compared with cases when there was no contact. There was no significant difference in ζ_G or f_G between plants measured in both conditions. In the wind, adjacent plants appeared to move collectively, giving no resistance to motion.

Measurements on 10 plants with both the ear upright and the ear down (no inter-row contact) showed that the peak in $|G_{MP}(f)|$ was 52% greater when the ear was upright than when it had fallen. The frequency of the peak location (f_G) was also shifted upward (Figure 6). For most frequencies, $|G_{MP}(f)|$ was decreased

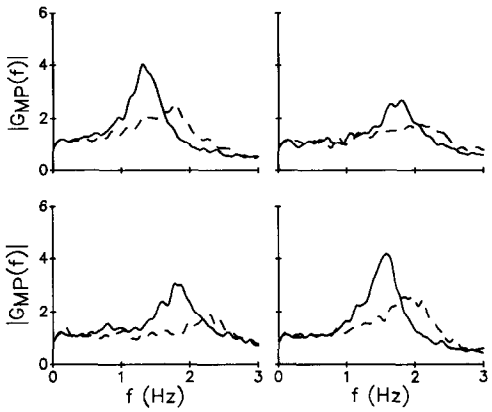

Fig. 6. A comparison of the measured transfer function ($|G_{MP}(f)|$) with frequency (f) for the upright (——) and down (-----) ear condition for four plants.

when the ear was down. This means less plant motion for a given wind energy when the ear was down.

Some change in motion characteristics was expected when the ear fell to a down position due to a lowering of the ear height. A reduction in ear height should increase ω_n, ζ, and K. For a 2.5 m tall plant with $E = 1.25$ m and $m_s = m_e = 0.5$ kg (with the corresponding $\zeta = 0.15$ and $\omega_n = 8.8\ \text{rad s}^{-1}$ or $f_n = 1.4$ Hz), a typical reduction in ear height of 0.25 m due to the ear falling to the down position corresponded to a calculated increase in ω_n and ζ of 9% and 8% (using Equations (8) and (9)). The increase in K was calculated to be 1.5% (using Equation (2)). Therefore, ear height alone can not explain the increase in ζ and ω_n, and the decrease in motion when the ear moves to a down position.

Upon closer examination, the assumption of a 1-DOF system is clearly violated when the ear is down and free to move. An oscillating stalk with a moving ear mass is a two degree-of-freedom (2-DOF) system. In a 2-DOF system with a main mass (stalk) and an auxiliary mass (ear), the motion of the main mass can be greatly influenced by the dynamic characteristics of the auxiliary mass. When the ω_n of the auxiliary mass is close to that of the main mass, it acts as a vibration absorber, reducing motion in the main mass by exerting a force which counteracts the inertial force of the main mass (Meirovitch, 1986).

The ω_m of a hanging ear was not measured, but can be estimated by assuming that the ear is a cylinder of length l and mass m_e, hanging freely by the shank (no friction). Ear motion (with no external forces) is described by

$$(m_n l^2/3)\,\ddot{\theta}_e - (m_e g l/2)\sin\theta_e = 0\,,$$

where θ_e is the angle that the ear axis makes with the vertical and $\ddot{\theta}_e$ is the angular acceleration of the ear. If the ear displacements is small (so that $\sin\theta_e \simeq \theta_e$), then ω_n is

$$\omega_n = [(m_e g l/2)/(m_e l^2/3)]^{1/2} = [1.5g/l]^{1/2} \quad (\text{rad s}^{-1}) .$$

Based on a m_e of 0.4 kg and an l of 0.25 m, the ω_n is 7.67 rad s^{-1}. This is just below ω_n values of the stalk. It appears that a free-hanging ear could act as a vibration absorber. This would partially explain the increase in the apparent ζ and f_n, and the reduction of $|G_{MP}(f)|$, when the ear moves to a down position (Figure 6).

3.5. Plant stiffness

The K_G represents the stiffness calculated from the transfer function while K_X and K_Y are directly measured stiffnesses. The two stiffness measures should be similar. A weighted average of K_X and K_Y(K_{XY}) was created based on the proportion of the total stalk displacement in each direction. Comparing the two measures of stiffness showed that K_G averaged 70% of K_{XY} (significantly different, $P = 0.1$).

It was expected that K_G would be larger, not smaller than K_{XY}. The K_{XY} was measured by applying a force directly on the stalk, while K_G was calculated from displacements caused by the wind force acting over the whole plant. Some of the wind force on the plant is likely to be dissipated in leaf motion and upper stalk motion which is not transferred to the lower stalk. Therefore the wind force required to displace a plant a given distance should be greater than a force applied directly at the stalk to give the same displacement: or K_G should be greater than K_{XY}.

Some difference in K_{XY} and K_G was likely due to incorrect assumptions made in estimating M_w. Of these assumptions (linear wind profile, LAD, C_{DL} and C_{DS}), the most likely to be in error is C_{DL}. Adjusting C_{DL} so that the average K_G equaled K_{XY} gave a value of 0.32. This is substantially higher than the 0.2 used to calculate M_w, and generally above literature values. There are two reasons to expect a higher C_{DL} than others have found. Most other estimates of C_{DL} have come from research done on leaves or canopies earlier in the season (Uchijima and Wright, 1963; den Hartog, 1973; Wilson *et al.*, 1982). Before senescence, corn leaves are flexible and the leaf area per unit land area is large. These factors promote streamlining and mutual sheltering of the leaves, which reduce C_{DL} (Thom, 1971). As the canopy senesces, the leaves become stiff and the plants lose leaf area. Therefore, an increase in C_{DL} would be expected. It was also observed that the upper leaves had a relatively vertical orientation. This would increase the C_{DL} (Thom, 1968) in the upper canopy. Since M_w is heavily weighted by the wind acting on the upper canopy, it seems probable that the difference in K_{XY} and K_G indicates a higher C_{DL} than was used. Another possible explanation for K_G being less than K_{XY} is a contribution of the tassel area to M_w, which was ignored in the calculations. At the plant top, momentum absorbed by the tassel may have a large effect on M_w. While the spike area of the tassel is very small (especially during senescence), the tassel might aerodynamically be an effective cylinder of quite

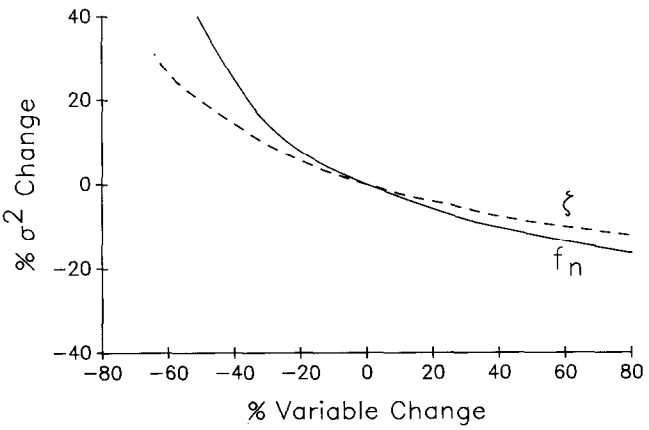

Fig. 7. The theoretical change in plant displacement variance (σ^2) for a given change in damping coefficient (ζ) and natural frequency (f_n). The results were based on a plant with an initial ζ of 0.15 and $\hat{a}$ f_n of 1.4 Hz ($\omega_n = 8.8$ rad s^{-1}), for the measured wind characteristics of Oct. 25.

some size much greater than the actual projected area of the tassel. Looking at spruce twigs, Grant (1983) found that at high velocity, the flow "sees" the twigs as solid cylinders, as opposed to a porous cylinder at low velocities. However, the foliage porosity of the tassel is small, much less than that of a spruce twig, and it seems unlikely that the tassel would "appear" as a large body at the observed wind speeds.

3.6. Theoretical effect of σ and f_n on motion

As a second-order system, plant motion in the wind will be influenced by ζ and f_n. Their effect on motion was examined by creating theoretical $S_P(f)$ functions for various ζ and f_n values using the $S_M(f)$ of Oct. 25 and the theoretical second-order transfer function (Equation (15)). Plant stiffness was not changed. Using the plant described in Section 3.4 as initial conditions (ζ of 0.15 and f_n of 1.4 Hz), the displacement variance of plant motion was determined by integrating $S_P(f)$ with f.

In theory, plant motion would increase with decreasing ζ and f_n. As ζ decreases, the peak in $|G_{MP}(f)|$ will increase, meaning greater displacements for wind energy at frequencies near f_n. Decreasing f_n increases motion by shifting the frequency peak in $|G_{MP}(f)|$ to frequencies of greater wind energy, giving greater magnitude resonant oscillations. Modeled plant motion showed this (Figure 7). Motion was relatively insensitive to f_n given the range of f_n observed in this study: -9 to $+58\%$ in terms of Figure 7. This range of f_n resulted in a change in modeled motion of $+4$ to -12%. Plant motion could become much more sensitive to f_n changes if f_n were lowered beyond this range. The effect of ζ on motion appears less than the effect of f_n from Figure 7, but the observed range of ζ (-37 to $+200\%$) resulted in a greater change in motion: from $+13$ to -30%. On the plants studied, ζ appears to have a greater effect on motion than f_n.

If the plant was better approximated by a flexible beam than a rigid rod, the flexure would result in the model overestimating the stiffness. Corresponding to this overestimate would be the overestimate of f_n and the underestimate of ζ. Therefore using the above theory for a 'flexible' stalk would cause a better alignment with the higher wind energy, giving greater predicted resonant motion. However, the stalk motion would be damped to a greater extent resulting in inconclusive effects of the presence of flexure in the stalk on the plant motion. Since the model used in this study did match the observed f_n reasonably well (e.g., Figure 5), we believe that the 'rigid rod' model sufficiently describes the corn stalks studied during senescence. Clearly the modelling of younger corn stalks may require the consideration of stalk flexure as the younger corn stalks are far more flexible than the dry senescent stalks.

4. Summary and Conclusions

The wind force on a corn plant in the field resulted in plant motion. The motion of the typical plant was characterized by resonant oscillation between 1 and 2 Hz. Transfer functions created from power spectra of the wind moment and plant displacement showed that lower stalk motion was generally well described by a second-order, single degree-of-freedom (1-DOF) response 'rigid rod' model. In theory, this means that plant motion in the wind can be described by its rotary stiffness (K), damping coefficient (ζ), and natural frequency (f_n) and that there was negligible bending of the stalk due to stalk flexibility.

Plant motion should increase as ζ increases and the frequency of an oscillating input force approaches f_n. Because wind energy decreased with increasing frequency, plant motion would be decreased by shifting f_n to higher frequencies. This was seen in the effect of ear position on motion. When the ear had fallen from an upright position, plant motion was significantly reduced. This reduction appears to be caused by the free hanging ear acting as a vibration absorber, increasing the effective ζ by 52%, and shifting f_n upwards by 22%.

The effect of ζ and f_n on plant motion suggests that lodging resistance in corn may be influenced by plant dynamic characteristics. Plants having relatively low ζ and f_n values would be expected to have a greater potential for lodging than plants with higher values.

References

Bearman, P. W.: 1971, 'Corrections for the Effect of Ambient Temperature Drift on Hotwire Measurements in Incompressible Flow', *DISA Information* **11**, 25–30.

Bloomfield, P.: 1976, *Fourier Analysis of Time Series: An Introduction*, John Wiley and Sons, Inc., New York, NY.

Daily, J. W. and Harleman, R. F.: 1966, *Fluid Dynamics*, Addison-Wesley Publishing Co. Inc., Reading, MA.

den Hartog, G.: 1973, 'A Field Study of the Turbulent Transport of Momentum Between the Atmosphere and a Vegetative Canopy', Ph.D. diss. Univ. of Guelph, Guelph, Ontario, Canada.

Finnigan, J. J.: 1979, 'Turbulence in Waving Wheat I. Mean Statistics and Honami', *Boundary-Layer Meteorol.* **16**, 181–211.

Finnigan, J. J. and Mulhearn, P. J.: 1978, 'A Simple Mathematical Model of Airflow in Waving Plant Canopies', *Boundary-Layer Meteorol.* **14**, 415–431.

Grant, R. H.: 1983, 'The Scaling of Flow in Vegetative Structures', *Boundary-Layer Meteorol.* **27**, 171–184.

Holbo, H. R., Corbett, T. C., and Horton, P. J.: 1980, 'Aeromechanical Behavior of Selected Douglas Fir', *Agric. Meteorol.* **21**, 81–91.

Inoue, E. 1955, 'Studies of Phenomena of Waving Plant (Honami) Caused by Wind. Part 1. Mechanism and Characteristics of Waving Plants Phenomena', *J. Agric. Meteorol. (Japan)* **11**, 87–89.

Jorgensen, F. E. 1971, 'Directional Sensitivity of Wire and Fiber Film Probes', *DISA Information* **11**, 31–37.

Maitani, T.: 1979, 'An Observational Study of Wind-Induced Waving of Plants', *Boundary-Layer Meteorol.* **16**, 49–65.

Maitani, T.: 1981, 'Measurements of Vibration of Rice Plants During the Period of Passaging Typhoon (7912) at Kurashiki Area', *J. Agric. Meteorol. (Japan)*. **36**, 251–255.

Meirovitch, L.: 1986, *Elements of vibration analysis*. McGraw-Hill Book Co., New York, NY.

Thom, A. S.: 1968, 'The Exchange of Momentum, Mass, and Heat Between an Artificial Leaf and the Airflow in a Wind-Tunnel', *Quart. J. Roy. Meteorol. Soc.* **94**, 44–55.

Thom, A. S. 1971, 'Momentum Absorption by Vegetation', *Quart. J. Roy. Meteorol. Soc.* **97**, 414–428.

Uchijima, Z. and Wright, J. L.: 1964, 'An Experimental Study of Air Flow in a Corn Plant-Air Layer', *Bull. National Inst. Agric. Sci. (Japan)* A-11.

Wilson, J. D., Ward, D. P., Thurtell, G. W., and Kidd, G. E.: 1982, 'Statistics of Atmospheric Turbulence Within and Above a Corn Canopy', *Boundary-Layer Meteorol.* **24**, 495–519.

Wilson, N. R. and Shaw, R. H.: 1977, 'A Higher Order Closure Model for Canopy Flow', *J. Appl. Meteorol.* **16**, 1197–1205.